Voltammetry and Electron-Transfer Dynamics in a Molecular Melt of a 1.2 nm Metal Quantum Dot

Dongil Lee, Robert L. Donkers, Joseph M. DeSimone, and Royce W. Murray*

Kenan Laboratories of Chemistry and NSF Science & Technology Center for Environmentally Responsible Solvents and Processes, University of North Carolina, Chapel Hill, North Carolina 27599-3290

Received October 21, 2002 ; E-mail: rwm@email.unc.edu

Gold nanoparticles have been the focus of numerous investigations in recent years because of promises offered by their optical, electronic, and chemical properties.[1] Au nanoparticles containing <200 down to a few tens of atoms are particularly interesting because they appear, from a variety of synthetic, spectral, and electrochemical observations,[2] to represent the bulk-to-molecule transition region where electronic band energetics yield to quantum confinement effects and discrete electronic states emerge. The barest outline of electronic properties of metal quantum dots has begun to emerge from these studies. Voltammetry of alkanethiolate-coated monolayer-protected metal clusters (MPCs)[3] has been reported[2d] for MPCs with 8−38 kDa core mass, and size-dependent opening of an energy gap at the Fermi level, representing molecular behavior, has been observed.[2c,d] The first explorations of electron-transfer dynamics of the larger (Au_{140}, 28 kDa) nanoparticles have been described.[4] This report provides the first results for the electron-transfer dynamics of the smallest, most molecular, member (8 kDa) of this transition.

Our investigations[5] of semisolid, redox polyether hybrid melts have shown that voltammetric charge transport measurements allow the evaluation of the redox electron hopping dynamics. In the interest of extending this capability to Au nanoparticles, we have prepared a polyether-based molten phase of a recently isolated and analytically characterized[6] very small Au nanoparticle **I** (relatively monodisperse, in nearly gram quantities) with a composition of $Au_{38}(PhC2)_{24}$, where PhC2 = phenylethylthiolate and TEM core diameter = 1.1 ± 0.3 nm. Knowing[7] that thiolated PEG chains (thiolated poly(ethyleneglycol), MW = 350, see the Supporting Information) can be place exchanged onto MPCs,[8] **I** was reacted with thiolated PEG ligands to produce a nanoparticle **II** having an estimated composition $Au_{38}(PhC2)_5(PEG)_{19}$ (Figure 1d). We will describe the dilute solution voltammetry of **I** and **II** and the electron-transfer dynamics between **II** and its oxidized forms in a semisolid, ionically conductive phase.

Exchange of the thiolated PEG ligand onto **I** was evaluated by transmission electron microscopy (TEM), NMR, UV−vis, and electrochemical comparisons of **I** with the product **II**. In the place exchange, ca. 80% of the original PhC2 ligands became replaced by thiolated PEG (^{1}H NMR analysis of **II**). TEM demonstrated that the average Au core diameter was substantially unchanged (~1.2 ± 0.4 nm, Supporting Information). The dilute solution UV−visible spectra (Supporting Information) of **I** and **II** are very similar to one another, with distinct steplike features as reported by Whetten et al.,[2c] and indicative of the emergence of discrete electronic energy states expected for very small nanoparticles. The fluid solution electrochemistries (differential pulse voltammetry, DPV) of **I** and **II** are also very similar (Figure 1a,b) to one another. Collectively, these comparisons show that the Au nanoparticle core size and electronic structure are substantially preserved in the synthesis of **II** from **I**. This result is significant encouragement, suggesting routes
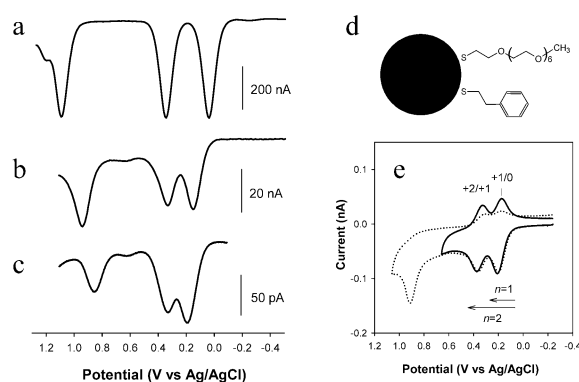

Figure 1. (a) 25 °C differential pulse voltammograms (DPVs) of 1.3 mM **I** in 0.1 M $Bu_4N^+PF_6^-$ in CH_2Cl_2, (b) 0.3 mM **II** in 0.1 M $Bu_4N^+PF_6^-$ in CH_3CN at 0.2 mm-radius Pt working, Ag/AgCl reference, and Pt coil counter electrode at 20 mV/s, and (c) **II$_{ion}$** melt containing $LiClO_4$ supporting electrolyte (16:1 ether oxygen:Li^+ ratio) as a semisolid film cast on 14 μm Pt microelectrode,[5] at 5 mV/s, 50 mV pulse. (d) Structures of thiolated PhC2 and PEG ligands passivating **I** and **II**. (e) 25 °C cyclic voltammograms of **II$_{ion}$** at 2 mV/s. Arrows indicate one- and two-electron potential steps performed in chronoamperometry experiments.

to other functionalized metal quantum dots from the synthetically accessible[6] **I**.

The voltammetry[2d,4a] of larger core size Au MPCs (i.e., Au_{140}) displays approximately evenly spaced peaks from Au_{140}^{3+} to Au_{140}^{3-} that correspond to serial changes of core charge by one oxidative or reductive electron transfers. The even peak spacing has been explained as a double layer charging phenomenon in which the core has a relatively constant capacitance. The voltammetry of **I** and **II** (Figure 1a,b) displays a pair of oxidation steps at ca. $+0.2$ and $+0.4$ V, followed at more positive potentials by further peaks (one of which is shown). The current peaks in Figure 1 are far from being uniformly spaced; the voltage separations are 0.30 and 0.75 V for **I** and 0.18 and 0.60 V for **II**. It is evident that the discretization and spacing of electronic levels of the Au_{38} core are qualitatively different from that of the Au_{140} nanoparticle.[2d,4a] Uneven voltage spacing of redox state changes is common for multivalent redox molecules, because of influences of HOMO−LUMO gaps, electronic coupling, and ligand−metal or metal−metal interactions, for example.[9] The electrochemical behavior of **I** and **II** is somewhat reminiscent of that reported[10] for the Pt cluster [Pt_{24}-$(CO)_{30}$].

$LiClO_4$ supporting electrolyte was dissolved in the PEG shell of **II** at a 16:1 ether oxygen:Li^+ ratio to create an ionically conductive nanophase around the Au_{38} nanoparticle (**II$_{ion}$**). The dissolution was accomplished by codissolving $LiClO_4$ and **II** in a fluid solvent, mixing well, and removing the solvent at reduced pressure until the nanoparticle phase **II$_{ion}$** was thoroughly dried. Using a 14 μm (diameter) microelectrode, we could observe voltammetry of **II$_{ion}$** in its undiluted state, as shown by DPV in Figure 1c and by cyclic
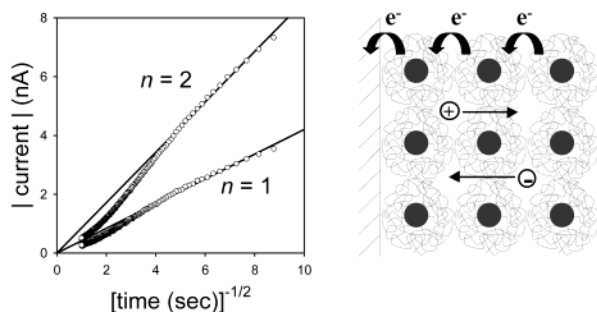
Figure 2. (a) Current (*i*) versus [time]$^{-1/2}$ responses (○) for $n = 1$ and $n = 2$ potential steps as shown in Figure 1e. Solid lines are linear regressions of short time, where the line intersects the origin as required by the Cottrell equation.[11] (b) Cartoon of electron hopping transport in a semisolid film of nanoparticle melts. Counterion movement is required to satisfy electroneutrality. MPC core and ligand size are roughly to scale.

voltammetry in Figure 1e. The two oxidation peaks at ca. +0.2 and +0.4 V are preliminarily assigned to the 1+/0 and 2+/1+ charge state charges of the Au_{38} core of **II**. These peaks are chemically reversible (they display oxidation and rereduction peaks of identical size) if the potential scan is halted before encompassing the more positive peak at +0.9 V. The voltage spacing between the three peaks is smaller (0.14 and 0.52 V) than that in fluid solution voltammetry. The product of the +0.9 V oxidation peak is in contrast somewhat unstable; the reduction peaks in Figure 1e were diminished because of the decomposition of the +0.9 V peak's product.

The Figure 1e voltammetry opens the way to estimate the rate of electron hopping between the nanoparticles of **II**$_{ion}$ using potential step chronoamperometry, using concepts previously developed[4a] for nanoparticles in network polymer films and for polyether redox melts.[5] Briefly, a potential step from ca. 0 to +0.3 V (Figure 1e) oxidizes **II** nanoparticles next to the electrode, which is followed by hopping of the electrode-injected holes from nanoparticle to nanoparticle through the **II**$_{ion}$ melt (Figure 2b). Supporting electrolyte counterions migrate concurrently, for electroneutrality. Because the electron hopping process is a diffusion-like phenomenon, the current−time response to the potential step follows the Cottrell equation,[11] which predicts a current proportional to [time]$^{-1/2}$. This is indeed seen in Figure 2a, and the electron diffusion coefficient D_E can be obtained from the slope of the linear portion of the plot. The slope of the plot is also proportional to the number of electrons in the electrode reaction; thus, stepping the potential across both nanoparticle oxidation waves (Figure 1e) doubles the slope ($n = 2$ vs $n = 1$), as seen in Figure 2a. At longer times, the Cottrell equation plot in Figure 2a exhibits a current drop-off, which is a finite diffusion effect arising from the limited thickness of the film of **II**$_{ion}$ that rests on the microelectrode, as has been observed before.[4a]

To calculate the electron hopping rates from D_E, we make the assumption that $D_E \gg$ the physical diffusion rate of **II** in the **II**$_{ion}$ melt. This is entirely reasonable based on our previous experience in semisolid polyether melts.[5] Thus, the rate constant for electron hopping between nanoparticles can be calculated from D_E (3.5 × 10^{-10} cm^2/s) obtained[12] in Figure 2a using[5,13]

$$D_E = k_{HOP}\delta^2/6 = k_{EX}\delta^2 C/6$$

where $\delta = 3.1$ nm[14] is the equilibrium center−center Au_{38} core separation and $C = 0.056$ M is the concentration[14] of cores in **II**$_{ion}$. The result (in first-order terms) is $k_{HOP} = 2.2 \times 10^4$ s^{-1}, and as a second order, self-exchange rate constant $k_{EX} = 3.8 \times 10^5$ M^{-1} s^{-1}. These values are smaller than those we have found in solid-state films of alkylthiolate and arylthiolate MPCs,[4b,c] but they are comparable with those in redox polymers[5] and network polymers of MPCs.[4a]

As noted above, these are the first results for molecule-like metal quantum dot electron-transfer dynamics. We do not attempt to interpret them at this time. The measured electron-transfer rates of **II** may reveal aspects of the semisolid environment of **II** that exert rate control. This is a question of current concern.[5] In any event, electron-transfer dynamics studies of molecule-like nanoparticles are highly relevant to their potential technological applications.

Voltammetry of a gold nanoparticle containing 11 core atoms was reported[15] after this manuscript was submitted.

Supporting Information Available: Preparative methods, UV− vis and TEM data for **II** (PDF). This material is available free of charge via the Internet at http://pubs.acs.org.

References

(1) (a) Schmid, G., Ed. *Clusters and Colloids*; VCH: Weinheim, 1994. (b) Hayat, M. A., Ed. *Colloidal Gold: Principles, Methods, and Applications*; Academic Press: San Diego, 1991.
(2) (a) Brown, L. O.; Hutchison, J. E. *J. Am. Chem. Soc.* **1997**, *119*, 12384. (b) Schmid, G. *Inorg. Synth.* **1990**, *27*, 214. (c) Schaaff, T. G.; Shafigullin, M. N.; Khoury, J. T.; Vezmar, I.; Whetten, R. L.; Cullen, W. G.; First, P. N.; Gutierrez-Wing, C.; Ascensio, J.; Jose-Yacaman, M. J. *J. Phys. Chem. B* **1997**, *101*, 7885. (d) Chen, S.; Ingram, R. S.; Hostetler, M. J.; Pietron, J. J.; Murray, R. W.; Schaaff, T. G.; Khoury, J. T.; Alvarez, M. M.; Whetten, R. L. *Science* **1998**, *280*, 2098. (e) Hakkinen, H.; Barnett, R. N.; Landman, U. *Phys. Rev. Lett.* **1999**, *82*, 3264.
(3) Templeton, A. C.; Wuelfing, W. P.; Murray, R. W. *Acc. Chem. Res.* **2000**, *33*, 27.
(4) (a) Hicks, J. F.; Zamborini, F. P.; Osisek, A. J.; Murray, R. W. *J. Am. Chem. Soc.* **2001**, *123*, 7048. (b) Wuelfing, W. P.; Green, S. J.; Pietron, J. J.; Cliffel, D. E.; Murray, R. W. *J. Am. Chem. Soc.* **2000**, *122*, 11465. (c) Wuelfing, W. P.; Murray, R. W. *J. Phys. Chem. B* **2002**, *106*, 3139.
(5) Lee, D.; Hutchison, J. C.; Leone, A. M.; DeSimone, J. M.; Murray, R. W. *J. Am. Chem. Soc.* **2002**, *124*, 9310.
(6) (a) Donkers, R. L.; Lee, D.; Murray, R. W., manuscript in preparation. (b) See the Supporting Information.
(7) Wuelfing, W. P.; Gross, S. M.; Miles, D. T.; Murray, R. W. *J. Am. Chem. Soc.* **1998**, *120*, 12696.
(8) Hostetler, M. J.; Green, S. J.; Stokes, J. J.; Murray, R. W. *J. Am. Chem. Soc.* **1996**, *118*, 4212.
(9) Ward, M. D. *Chem. Soc. Rev.* **1995**, *24*, 121.
(10) Roth, J. D.; Lewis, G. J.; Safford, L. K.; Jiang, X.; Dahl, L. F.; Weaver, M. J. *J. Am. Chem. Soc.* **1992**, *114*, 6159.
(11) Cottrell equation: $i = nFAD^{1/2}C/\pi^{1/2}t^{1/2}$, where n is the change in core charge state, C is the MPC concentration, and the other symbols are as commonly known.
(12) (a) D_E value is after migration correction.[12b] (b) Andrieux, C. P.; Saveant, J.-M. *J. Phys. Chem.* **1988**, *92*, 6761.
(13) Majda, M. In *Molecular Design of Electrode Surfaces*; Murray, R. W., Ed.; John Wiley & Sons: New York, 1992; pp 159−206.
(14) δ was determined from the average center-to-center core separation in the TEM image (Figure S2, Supporting Information), and the MPC concentration (0.056 M) was estimated on the basis of a cubic lattice relation $C = 1/\delta^3 N_A$, where N_A is Avogadro's number.
(15) Yang, Y.; Chen, S. *Nano Lett.* **2003**, *3*, 75−79.

JA029030N